HHS Public Access

Author manuscript

Genes Immun. Author manuscript; available in PMC 2011 October 01.

Published in final edited form as:

Genes Immun. 2011 April ; 12(3): 199–207. doi:10.1038/gene.2010.69.

Murine Lupus Susceptibility Locus *Sle2* Activates DNA-Reactive B Cells through Two Sub-Loci with Distinct Phenotypes

Leilani Zeumer[1], **Allison Sang**[1], **Haitao Niu**[1,2], and **Laurence Morel**[1]

[1] Department of Pathology, Immunology, and Laboratory Medicine, University of Florida, Gainesville, FL 32610

Abstract

The NZM2410-derived *Sle2* lupus susceptibility locus induces an abnormal B cell differentiation which most prominently leads to the expansion of autoreactive B1a cells. We have mapped the expansion of B1a cells to three *Sle2* sub-loci, *Sle2a*, *Sle2b*, and *Sle2c*. *Sle2* also enhances the breach of B cell tolerance to nuclear antigens in the 56R anti-DNA immunoglobulin transgenic (Tg) model. This study used the *Sle2* sub-congenic strains to map the activation of 56R Tg B cells. *Sle2c* strongly sustained the breach of tolerance and the activation of anti-DNA B cells. The production of Tg-encoded anti-DNA antibodies was more modest in *Sle2a* expressing mice, but *Sle2a* was responsible for the recruitment for Tg B cells to the marginal zone, a phenotype that has been found for 56R Tg B cells in mice expressing the whole *Sle2* interval. In addition, *Sle2a* promoted the production of endogenously encoded anti-DNA antibodies. Overall, this study showed that at least two *Sle2* genes are involved in the activation of anti-DNA B cells, and excluded more than two-thirds of the *Sle2* interval from contributing to this phenotype. This constitutes an important step toward the identification of novel genes that play a critical role in B cell tolerance.

Keywords

Lupus; B cells; autoantibodies; marginal zone; genetics

INTRODUCTION

Sle2 is one of three major quantitative trait loci that increase susceptibility to lupus nephritis in the NZM2410 mouse model[1]. Analysis of congenic strains combining these three loci on a C57BL/6 (B6) genetic background has shown that *Sle2* increased the frequency of fatal disease from 41% in B6.*Sle1*.*Sle3* to 98% in B6.*Sle1*.*Sle2*.*Sle3* mice[2]. *Sle2* expression on a B6 background is associated with a number of B cell defects, including an expansion of the

Correspondence: Dr. Laurence Morel, Department of Pathology, Immunology and Laboratory Medicine, University of Florida, Gainesville, FL 32610-0275. morel@ufl.edu.

[2]Current address: Center For Autoimmune and Musculoskeletal Disease, The Feinstein Institute for Medical Research, 350 Community Drive, Manhasset, NY 11030

Conflict of interest

The authors have no conflict of interest.

B1a cell compartment, especially in the peritoneal cavity (PerC). Using congenic recombinants, we have determined that the expansion of B1a cells mapped to three sub-locus, *Sle2a*, *Sle2b*, and *Sle2c*, with the major contribution provided by the telomeric *Sle2c*[3]. *Sle2* also increased production of polyreactive IgM antibodies (Ab)[4], which may be at least in part related to the expansion of the B1a cell compartment.

The 56R immunoglobulin heavy chain (HC) transgenic (Tg) anti-nuclear autoreactive B cells represent one of the best characterized models of B cell tolerance relevant to systemic lupus erythematosus (SLE) [5,6] Autoreactive anti-nuclear specificities are created by the pairing of the 56R HC (IgM^a allotype) with a number of endogenous light chains. Contrary to the BALB/c genetic background in which 56R Tg autoreactive B cells are effectively tolerized through at a variety of checkpoints, the B6 background is more permissive and induces the production of Tg-encoded anti-DNA Abs[7]. The breach of tolerance by 56R Tg B cells is greatly enhanced by the MRL/lpr lupus-prone genetic background[6]. *Sle2* also enhances the activation and differentiation of 56R Tg autoreactive B cells, in that B6.*Sle2*.56R mice produced significantly more Tg-encoded anti-DNA Abs than the B6.56R controls[8]. Furthermore, the activation of autoreactive 56R Tg B cells by *Sle2* involved their preferential recruitment to the marginal zone (MZ) compartment[8]. MZB cells in non-autoimmune mice are enriched for autoreactive specificities[9], and preferential recruitment to this compartment may represent a venue by which autoreactive B cells escape tolerance checkpoints.

The present study was conducted to map the activation of 56R Tg B cells within the *Sle2* locus using the sub-congenic strains that were produced to map the expansion of B1a cells[3]. We have found that *Sle2c*, and to a lesser extent *Sle2a*, expression enhanced the breach of tolerance of anti-DNA 56R Tg cells. Furthermore, we found that *Sle2a* but not *Sle2c* promoted the recruitment of autoreactive B cells to the MZ. Finally, *Sle2a* induced the activation and differentiation of B cells, including autoreactive ones, expressing endogenous HCs. Overall, these results showed that at least two gnes are involved in the *Sle2* activation of anti-DNA autoreactive B cells, and excluded more than two-thirds of the *Sle2* interval from contributing to this phenotype. This constitutes an important step toward the identification of novel genes that play a critical role in B cell tolerance to nuclear antigens.

RESULTS

Two *Sle2* sub-loci enhanced Ab production from 56R Tg B cells

Since their initial production and the characterization of their involvement in the accumulation of B1a cells[3], the *Sle2a* and *Sle2c* intervals have been fine-mapped (Fig. 1). *Sle2a* is now defined as a 1.5 – 4 Mb interval of NZW origin which contains a maximum of 24 expressed genes (Table 1) plus 16 additional predicted genes. The localization of *Sle2c* has been refined to a 10 –15 Mb NZB interval, and it is has been renamed *Sle2c1* to distinguish it from a more telomeric locus, *Sle2c2* (Xu et al., submitted). In this report, *Sle2c1* will be referred to as *Sle2c* for simplicity. The *Sle2b* interval in the central part of *Sle2* is the largest one and it potentially overlaps with *Sle2c* in their respective telomeric and centromeric recombination regions.

Activation of autoreactive 56R Tg B cells was first assessed by the presence of serum anti-DNA IgM Abs in the three sub-congenic strains as compared to B6.56R. Samples from B6.*Sle2*.56R were used as positive controls. B6.*Sle2a*.56R and B6.*Sle2c*.56R produced significantly more anti-ssDNA IgM than B6.56R mice, while there was no difference between B6.*Sle2b*.56R and B6.56R (Fig. 2A). Interestingly, both B6.*Sle2a*.56R and B6.*Sle2c*.56R produced significantly more anti-ssDNA IgM than B6.*Sle2*.56R mice ($p = 0.006$ and $p = 0.001$, respectively), suggesting that *Sle2* also contains a suppressive locus located outside the *Sle2a* and *Sle2c* regions. As expected, the majority anti-ssDNA IgM was of the Tg-encoded IgM^a allotype in B6.*Sle2*.56R and B6.*Sle2c*.56R mice (Fig. 2B). This was not the case, however, for B6.*Sle2a*.56R mice, in which the majority of anti-ssDNA IgM Abs carried the endogenous IgM^b allotype (Fig. 2C). Similar results were obtained for anti-dsDNA IgM (Fig. 2D–F), although B6.*Sle2a*.56R mice produced significantly more anti-dsDNA IgM^a Ab than B6.56R mice, but significantly less than B6.*Sle2c*.56R mice ($p = 0.01$). An ELISPOT analysis confirmed that the B6.*Sle2c*.56R splenocytes contained significantly more anti-ssDNA IgM^a Ab forming cells (AFCs) than B6.56R (Fig. 2G). On the other hand, B6.*Sle2a*.56R splenocytes contained significantly more anti-ssDNA IgM^b AFCs than B6.56R or any of the two other strains (Fig. 2I). These results show that the activation of 56R Tg autoreactive B cells maps to *Sle2c*, and to *Sle2a* to a lesser extent, with an additional contribution of *Sle2a* to the activation of endogenous HC autoreactive B cells.

To further characterize the activation of autoreactive B cells and to determine the respective contribution of the Tg versus endogenous HC, we compared the *in vitro* Ab secretion from splenic B cells, either spontaneously or after stimulation by LPS. B6.*Sle2c*.56R B cells spontaneously produced low but significantly higher levels of total IgM^a that B6.56R B cells (Fig. 3A), while B6.*Sle2a*.56R B cells spontaneously produced significantly more total IgM^b (Fig. 3B). IgG was undetectable in the supernatant of unstimulated cells (data not shown). As expected, LPS stimulation induced plasma cell differentiation and confirmed the results observed for serum IgM. Stimulated B6.*Sle2c*.56R B cells produced significantly more total IgM^a that B6.56R B cells (Fig. 3C). A higher level of total IgM^b was observed in all three *Sle2* strains, but the highest level was in B6.*Sle2a*.56R (Fig. 3D). Finally, B6.*Sle2*.56R and B6.*Sle2c*.56R B cells produced significantly more total IgG than B6.56R B cells, but the difference was not significant for B6.*Sle2a*.56R B cells (Fig. 3E). The *in vitro* production of anti-ssDNA IgM^a and IgM^b followed the same pattern as what we observed in serum samples (Fig. 3F–G). The different results obtained for total IgM^b and anti-ssDNA IgM^b indicate that both *Sle2a* and *Sle2c* enhanced Ab production by B cells carrying the endogenous HC, but only *Sle2a* supports the production of autoreactive Ab from these cells.

Sle2a induced the recruitment 56R Tg B cells to the MZB compartment and Sle2c increased their activation

The effect of the *Sle2* sub-loci expression on the distribution of peripheral B cells and their activation was analyzed by flow cytometry. A significantly higher ratio of perC B1a versus B2 IgM^a 56R Tg B cells was found in B6.*Sle2*.56R mice as compared to B6.56R mice (Fig. 4A). The perC B1a/B2 IgM^a 56R Tg B cell ratio was however similar between the three *Sle2* sub-congenic strains and B6.56R. As expected, the proportion of endogenous perC B cells with a B1a phenotype was much higher in B6.*Sle2*.56R than in B6.56R mice (Fig. 4B).

This was also the case for both B6.*Sle2a*.56R and B6.*Sle2c*.56R, although to a lower level than with the full interval. This confirmed that the *Sle2* sub-loci have additive effect to promote the recruitment of B cells into the B1a compartment, and that it also applied to Tg B cells.

All five 56R congenic strains showed similar splenocyte numbers (data not shown), percentages (Fig. 4C) and numbers (data not shown) of $B220^+$ cells, as well as percentages (Fig. 4D) and numbers (data not shown) of IgM^a Tg B cells (about 80% of the total B cells). The distribution of these splenic B cells differed however between strains. As previously reported, the MZB compartment was greatly expanded in the 56R strains (Fig. 4E, compare to non-Tg strains on the right of the graph), and this expansion was further enhanced by *Sle2* expression. Both *Sle2a* and *Sle2c* expression expanded the MZB compartment in 56R Tg mice (Fig. 4E), but only *Sle2a* was associated with the expansion of the 56R Tg IgM^a MZB subset that has been described for the whole *Sle2* interval[8]. Interestingly, in addition to be recruited more frequently to the MZ, total $B220^+$ IgM^a Tg B cells were also larger in B6.*Sle2a*.56R IgM^a than in the other 56R congenic strains (Fig. 4G). Finally, the increased activation of 56R Tg IgM^a B cells that has been described for B6.*Sle2*.56R mice[8] mapped to *Sle2c* and not *Sle2a*, as shown for both class II I-a^b (Fig. 4H) and CD86 (Fig. 4I). As for Ab production, the B cells in B6.*Sle2b*.56R mice were very similar to that of B6.56R, except for an increased I-a^b expression (Fig. 4H). This indicated that the *Sle2b* interval can be excluded from contributing to the activation of autoreactive B cells.

The effects of *Sle2a* expression on the recruitment of the 56R Tg B cells to the MZ was examined by histology. We used CD1d expression to differentiate $CDd1^{hi}$ MZB cells from $CD1d^{lo}$ follicular (FO) B cells, as this staining scheme has been validated in the NZM2410 model[10]. The MZ looked markedly expanded in size and cell density in B6.*Sle2a*.56R spleens as compared to either B6.56R or B6.*Sle2c*.56R (Fig. 5A). The B6.*Sle2a*.56R MZB cells were all from Tg origin with no B6.*Sle2a*.56R IgM^b cell being detected by histology in the MZ (data not shown). A morphometric analysis demonstrated that the MZ area contained significantly more B cells in B6.*Sle2a*.56R spleens than in either B6.56R or B6.*Sle2c*.56R spleens (Fig. 5B). The same result was obtained when the percentage of $CD1d^+$ B cells was computed (Fig. 5B). We have previously shown that the majority of the MZB cells are located inside the follicles in NZM2410 and B6.*Sle1*.*Sle2*.*Sle3* mice[10]. This was not the case for B6.*Sle2a*.56R mice in which the majority of $CD1d^{hi}$ B cells were located inside the MZ, outside the $Moma1^+$ macrophages (Fig. 5A and D). Furthermore, the proportion of $CD1d^+$ B cells that were located in the FO was not different between 56R strains (data not shown) indicating that *Sle2a* is not responsible for the NZM2410 intra-follicular location of the MZB cells. Finally, the percentage of $CD1d^-$ B cells was also elevated in the MZ of B6.*Sle2a*.56R mice (Fig. 5E). Overall, the results demonstrate that *Sle2a* expression greatly enhances the recruitment of autoreactive B cells to the MZB compartment, considering either lineage marker expression or tissue location.

DISCUSSION

The mechanisms by which B cell tolerance is maintained in normal individuals but breached in autoimmune conditions has been of a great interest to immunologists. Most of the studies

have used B cell receptor transgenic mouse models and a number of checkpoints have been defined from these studies[6]. The well-documented effect of genetic background on the enforcement of these tolerance checkpoints implies that natural genetic variation regulates the fate of autoreactive B cells. Very little is known, however, on the identity of the genes that are involved. The *lpr* mutation that impairs *Fas* expression has been the first documented natural genetic variation that regulates B cell tolerance[11]. Very little progress has been made since with mouse models. In humans, recent progress has been made with recent association between the presence of autoAbs and loss-of-function rare variants of the sialic acid acetylesterase (*SIAE*) gene[12] or specific common alleles of the IRF7/PHRF1 locus[13].

We have used a congenic dissection approach to identify the genes responsible for lupus susceptibility in the NZM2410 model[14], and we have identified two SLE-susceptibility loci, *Sle1* and *Sle2*, that regulate B cell tolerance. Within *Sle1*, *Sle1b* regulates B cell tolerance to chromatin[15]. The double Tg HEL model[16] has demonstrated that *Sle1b* impairs B cell tolerance, and differential expression of splice isoforms of *Ly108*, a gene located in the *Sle1b* interval, were shown to regulate the deletion of autoreactive immature B cells[17]. These results have identified *Ly108* as a novel gene that regulates B cell tolerance to nuclear antigens. *Sle2* affects B cell development and functions in a B cell intrinsic manner[4],[18]. Its involvement in B cell tolerance was formally demonstrated with the 56H HC Tg model[8]. Therefore, the B6.*Sle2*.56R strain represents a good model to indentify the genes in the *Sle2* locus that amplify the breach of tolerance to nuclear antigens. We have already identified three regions *in Sle2*, *Sle2a*, *Sle2b*, and *Sle2c*, that contribute to B1a cell expansion[3]. B1a cells are the major source of natural Abs and their repertoire is intrinsically autoreactive[19]. It is therefore possible that the same genetic variations regulate B1a cell numbers and B cell tolerance. We have assessed Ab production, B cell distribution and activation, and splenic histology to analyze the fate of B cells in B6.*Sle2a*.56R, B6.*Sle2b*.56R, and B6.*Sle2c*.56R mice. These approaches concurred in identifying *Sle2c* and *Sle2a* as being responsible for the breach of tolerance of 56R Tg autoreactive B cells. The *Sle2c* interval induced the production of Tg-encoded anti-DNA Ab to a level similar or higher than the whole interval, as well as the activation of 56R Tg B cells. This identified *Sle2c* as the major contributor to B cell breach of tolerance within *Sle2*. The interval that we used in this study is large (~ 24 Mb), with too many genes to consider a candidate gene approach. We have produced *Sle2c* recombinants to map the B1a cell expansion and identified a mutation in the promoter of the *Cdkn2c* gene that greatly reduces the expression of this cell cycle inhibitor and is associated by B1a cell expansion (Xu et al. submitted). One may hypothesize that defects in cell cycle regulation may affect the fate of autoreactive B cells as it has been shown for genes regulating apoptosis[6]. The *Sle2c* recombinants will be used to further map the activation of the 56R Tg B cells and determine if it co-localizes with B1a cell expansion.

The involvement of *Sle2a* in 56R Tg B cell activation and differentiation is more complex. The production of Tg-encoded anti-DNA Ab in *Sle2a*-expressing mice is intermediate between that of B6.*Sle2c*.56R and B6.56R mice. However, *Sle2a* is clearly the locus that drives the selection of the 56R Tg B cells to the MZB cell compartment. This MZB cell selection is not sufficient to recapitulate the entire *Sle2* phenotype for 56R Tg B cells,

indicating that once the autoreactive B cells are selected to the MZ, another step is necessary to fully activate them. B1a cells and MZB cells are functionally related and are both enriched for autoreactive specificities[20], suggesting that the same gene might be responsible for the expansion of both compartments. One can hypothesize that the presence of the 56R HC Tg polarizes the B cell selection away from the B1a cell to the MZB cell compartment, but the molecular mechanism is the same. In addition, *Sle2a* was surprisingly associated with the differentiation of B cells producing total and anti-DNA Ab carrying endogenous HCs. Further experiments will be necessary to determine if this phenotype results from early bone-marrow selection events or a differential peripheral expansion of Tg versus endogenous HC clones. It is not possible to determine at this point whether the two major *Sle2a* phenotypes, MZB expansion and preferential endogenous HC activation, are regulated by the same gene. None of the *Sle2a* genes represents an obvious candidate gene (Table 1), and there are a large number of uncharacterized expressed sequences and predicted genes, indicating that a systematic approach will be necessary to indentify the causative gene.

The *Sle2b* interval was associated with a modest contribution to the B1a cell expansion[3], and we have shown here that it is not involved in the activation of anti-nuclear autoreactive B cells. This region is of interest because it contains the *Ifna* gene cluster, and we have shown that a lower expression of type 1 interferons in B6.*Sle2* mice was associated with increased autoAb levels and B1a cell numbers[21]. Our results with the 56R Tg model indicate that this is unrelated to the activation of anti-nuclear autoreactive B cells.

Overall, we have determined that at least two genes are responsible for the *Sle2* activation of anti-nuclear autoreactive B cells and have greatly reduced the genomic location of these two genes to a third of the original whole interval. None of the genes located in either of the two loci have a known involvement in B cell tolerance, which ensures that this study will lead to the discovery of new mechanisms of B cell tolerance.

MATERIALS AND METHODS

Mice

The B6.*Sle2* and B6.*Sle2* sub-congenic strains have been previously described[14],[3]. The termini of the *Sle2a* and *Sle2c1* intervals were mapped with a panel of SNPs that are polymorphic between NZW and B6, and NZB and B6, respectively (Fig. 1). SNP genotyping was performed by direct sequencing. B6 mice were originally obtained from the Jackson Laboratories. B6.*Sle2*.56R and B6.56R breeders were obtained from Dr. Chandra Mohan, (UTSW). B6.*Sle2a*.56R, B6.*Sle2b*.56R, and B6.*Sle2c*.56R were produced by intercrossing the corresponding B6.*Sle2* sub-congenic strains to B6.56R and by selecting for homozygozity at the termini shown in Fig. 1 and the presence of the 56R HC Tg as previously reported[22]. Mice used in this study were males and females aged between 9 and 12 mo of age. All experiments were conducted according to protocols approved by the University of Florida Institutional Animal Care and Use Committee.

Antibody measurements

Total IgM and IgG was measured as previously described[23]. Total IgM^a or IgM^b was detected in plates coated with goat anti-κ and revealed by polyclonal rabbit anti-IgM^a or IgM^b (Nordic Immunological Labs) followed by goat anti-rabbit-AP (Sigma-Aldrich). Anti-ssDNA and dsDNA IgM, IgM^a or IgM^b were detected in the same fashion on plates coated with dsDNA or heat-denatured ssDNA (50 μg/ml), as previously described[24]. Serum dilutions were 1:5,000 for total IgM, IgG, IgM^a or IgM^b, and 1:500 for anti-DNA IgM, IgM^a or IgM^b. *In vitro* Ab secretion was measured from magnetic bead-purified $CD43^-$ B cells (10^5 per well) cultured in complete RPMI 1640 (Cellgro) containing 10% FCS with or without 5 ug/ml LPS (Sigma) for 5 d. Ab levels were measured by ELISA in supernatants diluted 1:10 for unstimulated cells and 1:100 for LPS stimulated cells. ELISPOTs were performed as previously described[24]. Briefly, cells serially diluted in RPMI 1640 supplemented with 5% FCS were incubated on multiscreen filter plates (Millipore) coated with ssDNA for 5–7 h at 37°C. Bound secreted Ab was detected with polyclonal rabbit anti-IgM^a or IgM^b followed by goat anti-rabbit-AP. AFCs were counted using a Bioreader 4000 Pro-x (Bio-Sys).

Flow cytometry

PerC lavages or RBC-depleted splenocytes were stained as previously described[23] with the following conjugated mAbs or their isotype controls, purchased from BD Biosciences or eBioscience: AA4.1 (CD93), B220 (RA3-6B2), CD5 (53–7.3) CD23 (B3B4), CD86 (GL1), CD138 (281–2), IgM^a (DS-1), IgM^b (AF6-78) and $I\text{-}A^b$ (AF6). The 7E9 Ab was used to detect both NZW and B6 alleles of CD21[25]. Stained cells (100,000 per sample) were analyzed on a FACSCalibur™ (BD Biosciences, Mountain View, CA), and dead cells were excluded based on forward and side scatter characteristics.

Histology

Immunofluorescence staining was performed on frozen sections as previously described[26], with Moma-1-FITC (Serotec), CD1d-PE (1B1), and IgM^a-Biotin-SA-PB or B220-PB (RA3-6B2). Quantitation of the number and location of the cells with MetaMorph 7.5 image analysis was performed by a single operator without knowledge of the samples' identities. For each mouse, the numbers of $CD1d^+$ $B220^+$ cells and $CD1d^-$ $B220^+$ selected on each side of the Moma-1^+ ring were computed for one or two representative follicles with homogeneous staining on 100X amplification images.

Statistical analysis

Unpaired one-tailed t tests, or Mann-Whitney tests when the data were not distributed normally, were used to compare the B6.56R and the B6.*Sle2.56R* congenic mice. Dunnett's multiple comparison tests were used when appropriate. Data was analyzed with Graphpad Prism 4.0 software. Means, the standard errors of the mean (SEM), and the levels of statistical significance (*: $P < 0.05$, **: $P < 0.01$; ***: $P < 0.001$) are shown in the figures.

Acknowledgments

This work was supported by a National Institutes of Health grant RO1 AI068965 to LM. We thank Dr. Chandra Mohan for the generous gift of B6.56R and B6.Sle2.56R breeders, Xuekun Su for outstanding animal care, and members of the Morel lab for stimulating discussions.

Abbreviations used in this paper

B6	C57BL/6
perC	peritoneal cavity
Ab	antibody
HC	immunoglobulin heavy chain
Tg	transgene
SLE	systemic lupus erythematosus
AFC	antibody forming cell
MZ	marginal zone
FO	follicular

References

1. Morel L, Rudofsky UH, Longmate JA, Schiffenbauer J, Wakeland EK. Polygenic control of susceptibility to murine systemic lupus erythematosus. Immunity. 1994; 1:219–229. [PubMed: 7889410]
2. Morel L, Croker BP, Blenman KR, Mohan C, Huang G, Gilkeson G, et al. Genetic reconstitution of systemic lupus erythematosus immunopathology with polycongenic murine strains. Proc Natl Acad Sci U S A. 2000; 97:6670–6675. [PubMed: 10841565]
3. Xu Z, Duan B, Croker BP, Wakeland EK, Morel L. Genetic dissection of the murine lupus susceptibility locus *Sle2*: contributions to increased peritoneal B-1a cells and lupus nephritis map to different loci. J Immunol. 2005; 175:936–943. [PubMed: 16002692]
4. Mohan C, Morel L, Yang P, Wakeland EK. Genetic dissection of systemic lupus erythematosus pathogenesis - Sle2 on murine chromosome 4 leads to B cell hyperactivity. J Immunol. 1997; 159:454–465. [PubMed: 9200486]
5. Erikson J, Radic MZ, Camper SA, Hardy RR, Carmack C, Weigert M. Expression of anti-DNA immunoglobulin transgenes in non-autoimmune mice. Nature. 1991; 349:331–334. [PubMed: 1898987]
6. Fields ML, Erikson J. The regulation of lupus-associated autoantibodies: immunoglobulin transgenic models. Curr Opin Immunol. 2003; 15:709–717. [PubMed: 14630207]
7. Fukuyama H, Nimmerjahn F, Ravetch JV. The inhibitory Fc receptor modulates autoimmunity by limiting the accumulation of immunoglobulin G+ anti-DNA plasma cells. Nat Immunol. 2005; 6:99–106. [PubMed: 15592473]
8. Liu Y, Li L, Kumar KR, Xie C, Lightfoot S, Zhou XJ, et al. Lupus susceptibility genes may breach tolerance to DNA by impairing receptor editing of nuclear antigen-reactive B cells. J Immunol. 2007; 179:1340–1352. [PubMed: 17617627]
9. Bendelac A, Bonneville M, Kearney JF. Autoreactivity by design: innate B and T lymphocytes. Nat Rev Immunol. 2001; 1:177–186. [PubMed: 11905826]
10. Duan B, Niu H, Xu Z, Sharpe AH, Croker BP, Sobel ES, et al. Intrafollicular location of marginal zone/CD1d^{hi} B cells is associated with autoimmune pathology in a mouse model of lupus. Lab Invest. 2008; 88:1008–1019. [PubMed: 18607347]

11. Rathmell JC, Cooke MP, Ho WY, Grein J, Townsend SE, Davis MM, et al. Cd95 (Fas) Dependent Elimination of Self-Reactive B-Cells Upon Interaction with Cd4(+) T-Cells. Nature. 1995; 376:181–184. [PubMed: 7603571]
12. Surolia I, Pirnie SP, Chellappa V, Taylor KN, Cariappa A, Moya J, et al. Functionally defective germline variants of sialic acid acetylesterase in autoimmunity. Nature. 2010; 466:243–247. [PubMed: 20555325]
13. Salloum R, Franek BS, Kariuki SN, Rhee L, Mikolaitis RA, Jolly M, et al. Genetic variation at the IRF7/PHRF1 locus is associated with autoantibody profile and serum interferon-alpha activity in lupus patients. Arthritis Rheum. 2010; 62:553–561. [PubMed: 20112359]
14. Morel L, Mohan C, Yu Y, Croker BP, Tian N, Deng A, et al. Functional dissection of systemic lupus erythematosus using congenic mouse strains. J Immunol. 1997; 158:6019–6028. [PubMed: 9190957]
15. Morel L, Blenman KR, Croker BP, Wakeland EK. The major murine systemic lupus erythematosus susceptibility locus, Sle1, is a cluster of functionally related genes. Proc Natl Acad Sci U S A. 2001; 98:1787–1792. [PubMed: 11172029]
16. Cornall RJ, Goodnow CC, Cyster JG. The regulation of self-reactive B cells. Current Opinion in Immunology. 1995; 7:804–811. [PubMed: 8679124]
17. Kumar KR, Li L, Yan M, Bhaskarabhatla M, Mobley AB, Nguyen C, et al. Regulation of B cell tolerance by the lupus susceptibility gene Ly108. Science. 2006; 312:1665–1669. [PubMed: 16778059]
18. Xu Z, Butfiloski EJ, Sobel ES, Morel L. Mechanisms of peritoneal B-1a cells accumulation induced by murine lupus susceptibility locus Sle2. J Immunol. 2004; 173:6050–6058. [PubMed: 15528340]
19. Berland R, Wortis HH. Origins and functions of B-1 cells with notes on the role of CD5. Ann Rev Immunol. 2002; 20:253–300. [PubMed: 11861604]
20. Martin F, Oliver AM, Kearney JF. Marginal zone and B1 B cells unite in the early response against T-independent blood-borne particulate antigens. Immunity. 2001; 14:617. [PubMed: 11371363]
21. Li J, Liu Y, Xie C, Zhu J, Kreska D, Morel L, et al. Deficiency of type I interferon contributes to Sle2-associated component lupus phenotypes. Arthritis Rheum. 2005; 52:3063–3072. [PubMed: 16200585]
22. Chen C, Nagy Z, Radic MZ, Hardy RR, Huszar D, Camper SA, et al. The site and stage of anti-DNA B-cell deletion. Nature. 1995; 373:252–255. [PubMed: 7816141]
23. Niu H, Sobel ES, Morel L. Defective B-cell response to T-dependent immunization in lupus-prone mice. Eur J Immunol. 2008; 38:3028–3040. [PubMed: 18924209]
24. Mohan C, Alas E, Morel L, Yang P, Wakeland EK. Genetic dissection of SLE pathogenesis - Sle1 on murine chromosome 1 leads to a selective loss of tolerance to H2A/H2B/DNA subnucleosomes. J Clin Invest. 1998; 101:1362–1372. [PubMed: 9502778]
25. Boackle SA, Holers VM, Chen XJ, Szakonyi G, Karp DR, Wakeland EK, et al. Cr2, a candidate gene in the murine Sle1c lupus susceptibility locus, encodes a dysfunctional protein. Immunity. 2001; 15:775–785. [PubMed: 11728339]
26. Duan B, Croker BP, Morel L. Lupus resistance is associated with marginal zone abnormalities in an NZM murine model. Lab Invest. 2007; 87:14–28. [PubMed: 17170739]

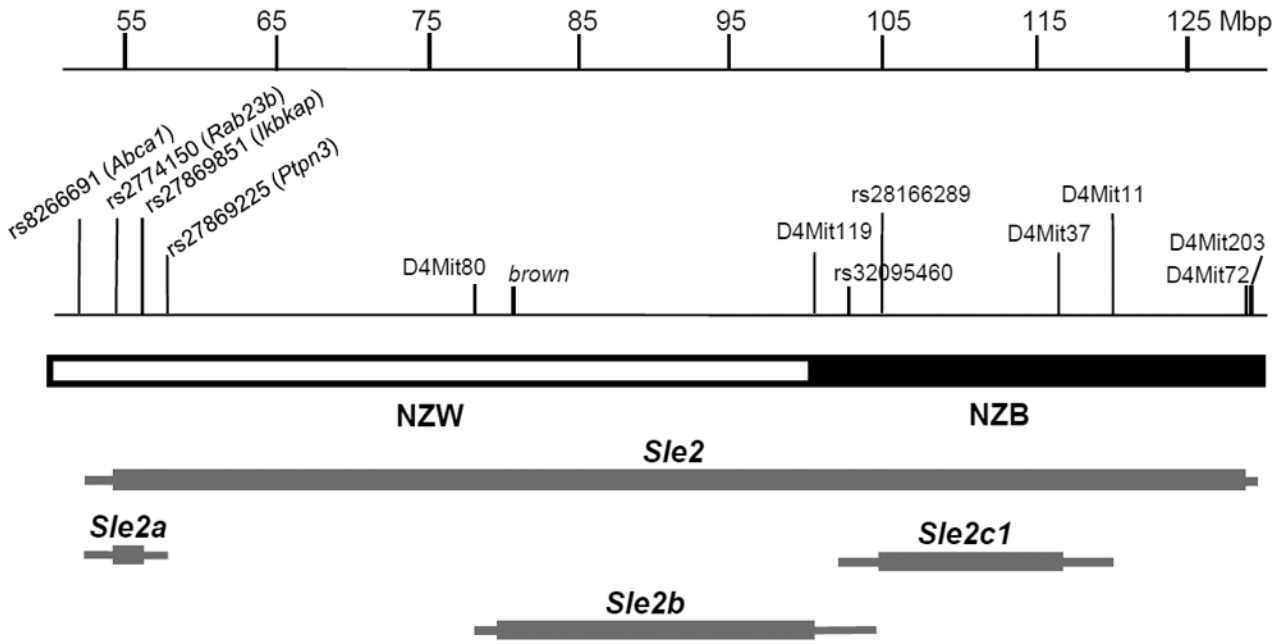

FIGURE 1.

Genetic map of the *Sle2* congenic strains used in this study. The location of the markers defining the termini of each recombinant is indicated on the top. The NZB/NZW derivation of the region is also shown. NZM2410 (NZW or NZB)-derived intervals are indicated by solid boxes, with the area of recombination between the NZM2410 and B6 genomes indicated by lines on each side. The location of each marker corresponds to the NCBIM37 built. For SNPs located within a known gene, this gene is indicated in parenthesis.

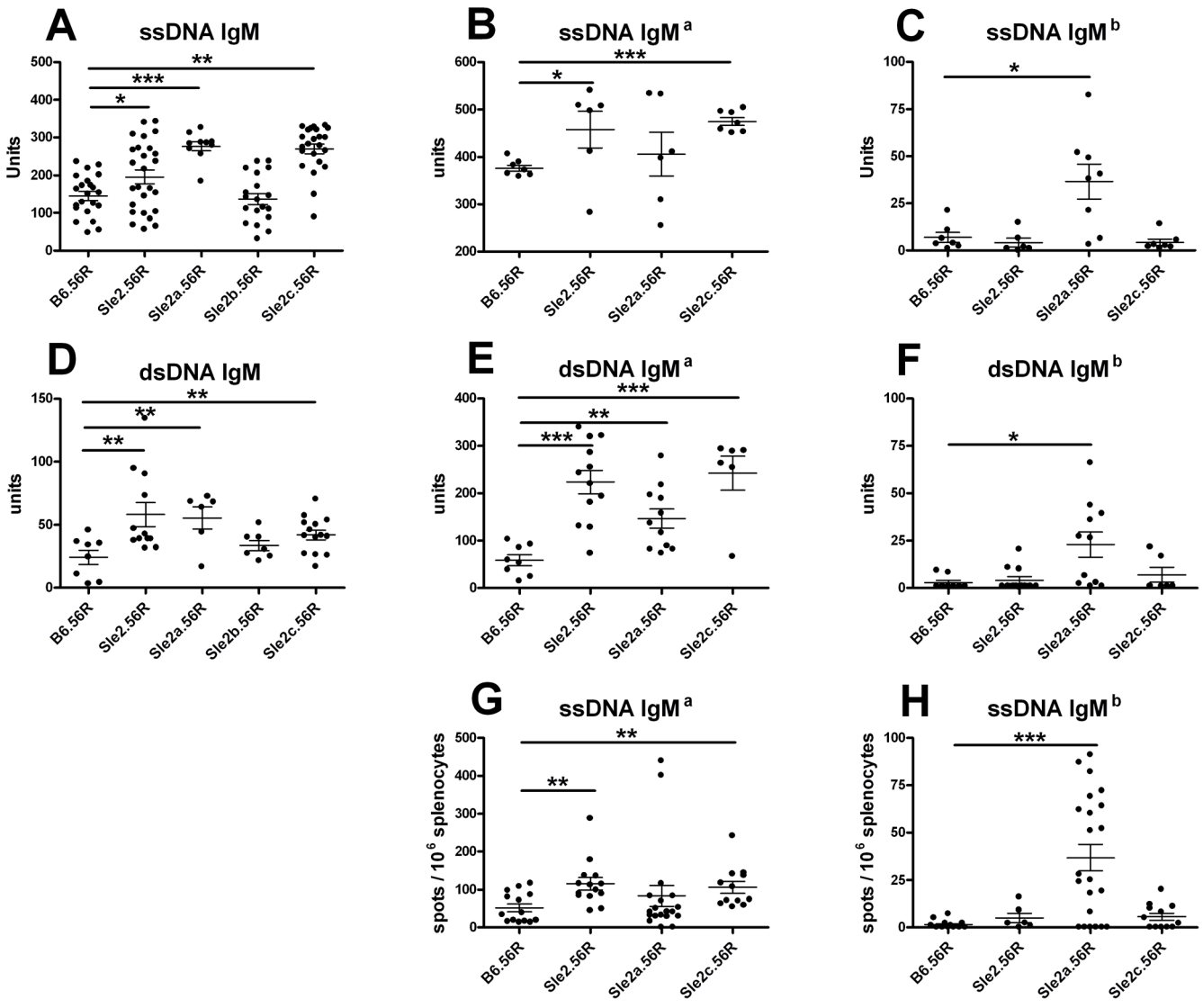

FIGURE 2.

Two *Sle2* sub-loci activate 56R B cells to produce anti-DNA Ab. Serum anti-ssDNA (**A**–**C**) and anti-dsDNA (**D**–**F**) IgM, with the left panels showing total IgM, the middle panels 56R Tg-encoded IgM^a, and the right panels endogenous IgM^b. **G**–**F**. Splenic anti-ssDNA IgM^a and IgM^b AFCs. Each data point represents one mouse.

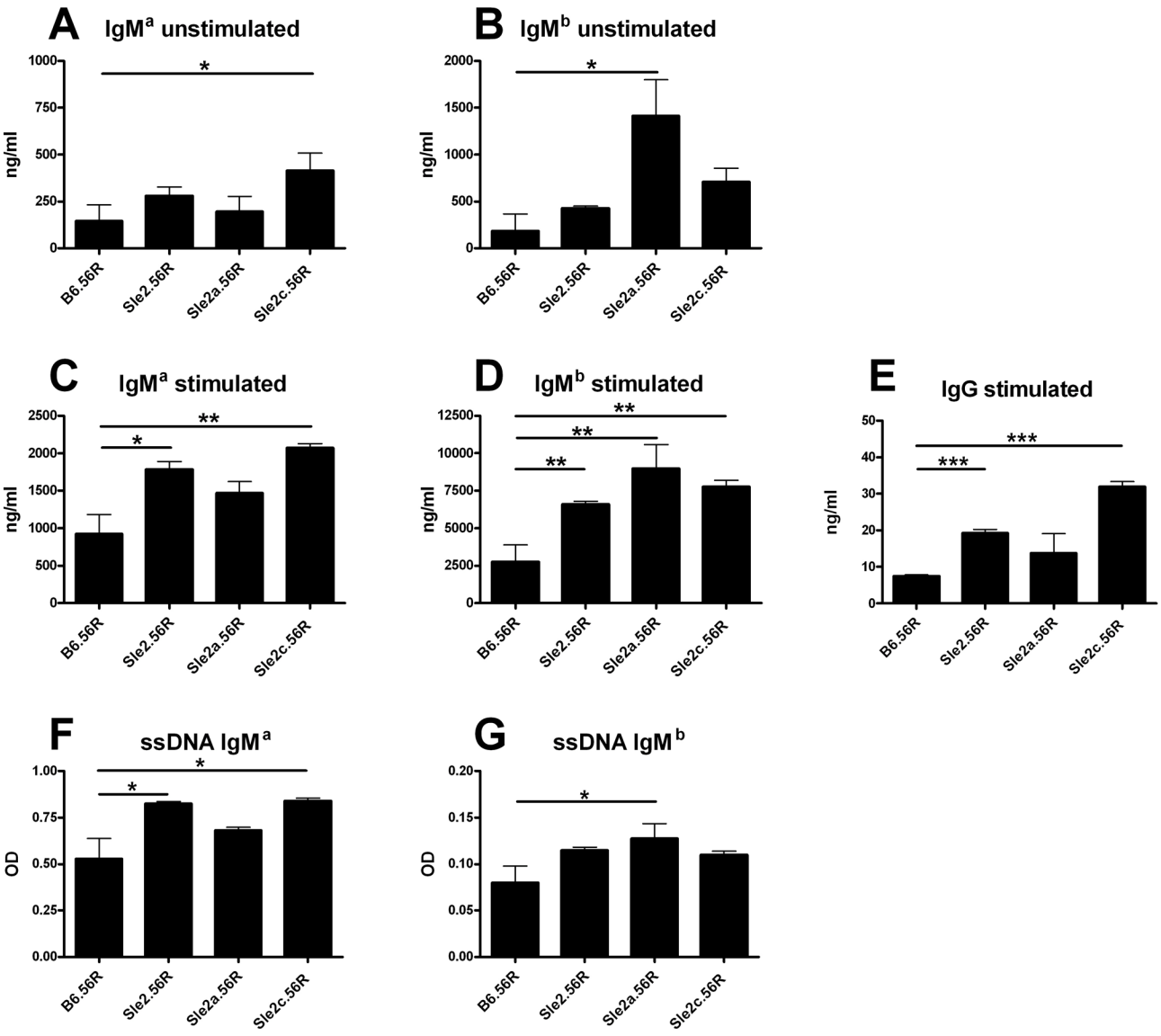

FIGURE 3.

In vitro Ab production in the B6.*Sle2*.56R congenic strains. Total Ig and anti-ssDNA IgM[a] or IgM[b] were measured in the supernatant of splenocytes cultured for 5 d without (**A**–**B**) or with 5 ug/ml LPS (**C**–**G**). Total IgM[a] (**A**) and IgM[b] (**B**) in the supernatant of unstimulated cells. Total IgM[a] (**C**), IgM[b] (**D**) and IgG (**E**) in the supernatant of LPS-stimulated cells. Anti-ssDNA IgM[a] (**F**) and IgM[b] (**G**) in the supernatant of LPS-stimulated cells. Graphs show means and SEM of 4–6 mice per strain.

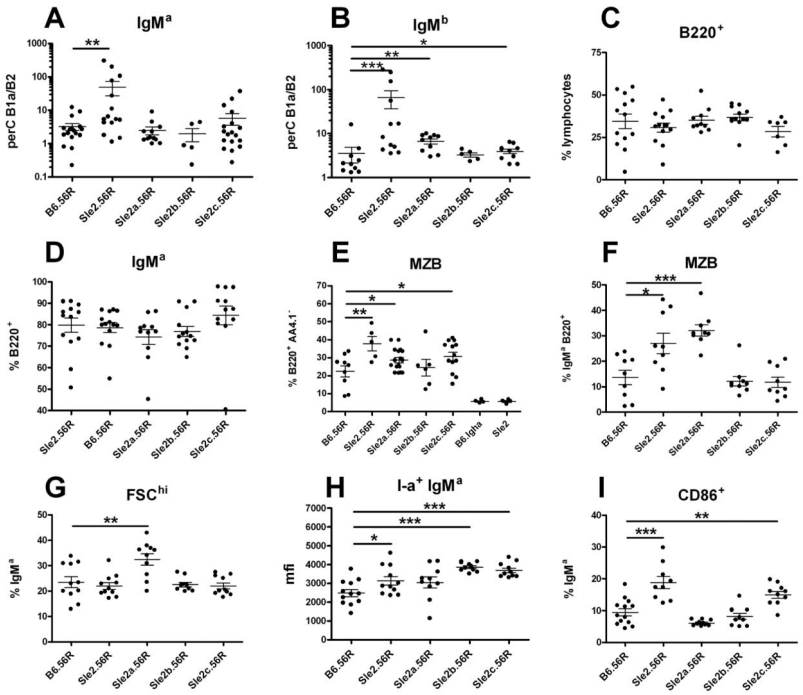

FIGURE 4.

Flow cytometric analysis of B cells in the B6.*Sle2*.56R congenic strains. **A**–**B**. PerC B1a/B2 cell ratios with B1a cells defined as $B220^{int}$ $CD5^{+}$ and B2 cells defined as $B220^{hi}$ $CD5^{-}$. The graph in **A** shows the ratios for cells gated on IgM^{a} and the graph in **B** for the cells gated on IgM^{b}. **C**–**I**. Analysis of splenic B cells. Percentage of total $B220^{+}$ cells (**C**) and IgM^{a+} $B220^{+}$ cells (**D**). **E**. Total $CD21^{hi}$ $CD23^{-}$ MZB cells expressed as the percentage of $AA4.1^{-}$ $B220^{+}$ mature B cells. **F**. Tg MZB cells expressed as the percentage of IgM^{a+} $B220^{+}$ cells. **G**. Percentage of large (FSC^{hi}) IgM^{a+} $B220^{+}$ B cells. **H**. Class II MHC I-a^{b} expression, measured as geometric mean fluorescence intensity (mfi) on IgM^{a+} B cells. **I**. Percentage of $CD86^{+}$ IgM^{a+} B cells.

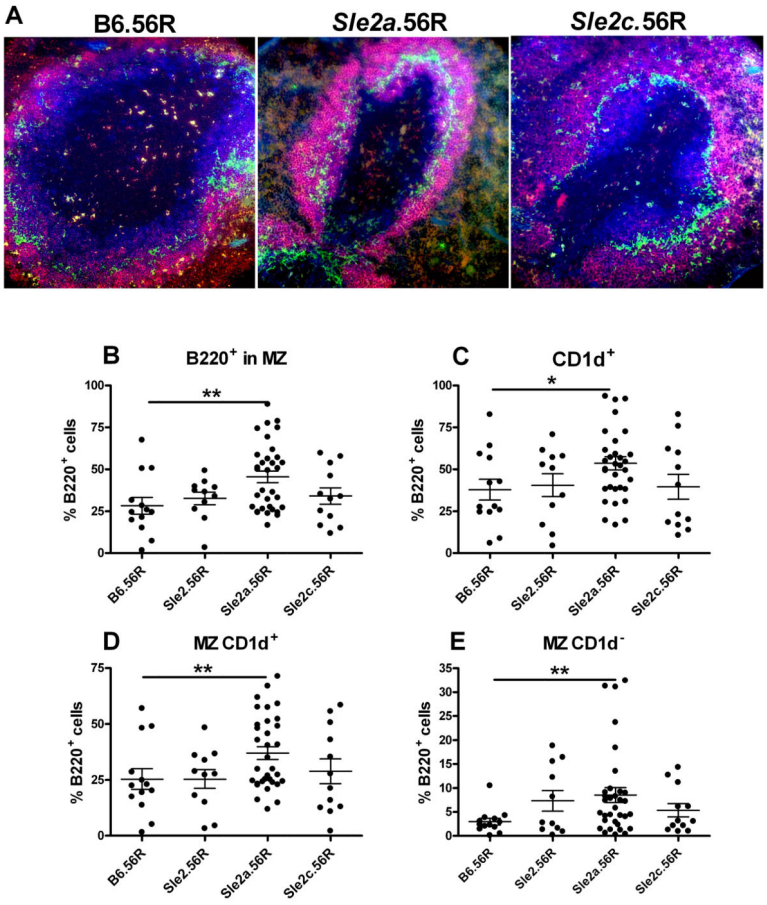

FIGURE 5.

Sle2a promotes the expansion of MZB cells in 56R Tg mice. **A**. Representative follicles from B6.56R, B6.*Sle2a*.56R, and B6.*Sle2c*.56R spleen sections. B220-PB (blue) and CD1d-PE (red) identify $B220^{+}$ $CD1d^{hi/+}$ magenta MZB cells and $B220^{+}$ $CD1d^{lo/-}$ blue FOB cells, and their location relative to Moma-1-FITC (green)-stained metallophilic macrophages that separate the MZ from the FO zones. Note the intensity of CD1d expression in the B6.*Sle2a*. 56R specimen. **B**. Proportion of $B220^{+}$ B cells located in the MZ outside of the Moma-1^{+} ring. **C**. Proportion of $B220^{+}$ B cells that expressed $CD1d^{hi/+}$ regardless of their location. **D**. Proportion of $B220^{+}$ B cells in the MZ that are $CD1d^{hi/+}$. **E**. Proportion of $B220^{+}$ B cells in the MZ that are $CD1d^{lo/-}$. Each data point corresponds to a representative follicle from one mouse from the indicated strains.

Table 1
List of expressed genes in the *Sle2a* interval

The shaded rows show the genes of known NZW derivation, flanked by the region of recombination between the NZW and B6 genomes on each side.

Genome coordinates[1]	Gene	B cell expression[2]
53043659-53172767 (−)	*Abca1*	++
53217938-53230729 (−)	*4930412L05Rik*	nt
53259068-53263987 (+)	*4930522O17Rik*	nt
53275604-53283104 (−)	*AI427809*	nt
53453285-53635350 (+)	*Slc44a1*	−
53575855-53577569 (−)	*1700060J05Rik*	nt
53644343-53719881 (+)	*Fsd1l*	+
53726870-53778657 (+)	*Fktn*	low
53792577-53801584 (+)	*Tal2*	+
53838917-53874891 (+)	*Tmem38b*	−
53873524-53873642 (+)	*n-R5s185*	nt
54957920-55096435 (+)	*Zfp462*	+
55362915-55405109 (+)	*Rad23b*	+
55540015-55545338 (−)	*Klf4*	−
56233489-56237393 (−)	*2310081O03Rik*	nt
56752877-56754315 (−)	*Actl7b*	−
56756285-56757797 (+)	*Actl7a*	−
56762552-56815203 (−)	*Ikbkap*	+
56815217-56822473 (+)	*BC026590*	nt
56823807-56878060 (−)	*Ctnnal1*	−
56879795-56960309 (−)	*D730040F13Rik*	nt
56970045-57003263 (−)	*6430704M03Rik*	nt
57004844-57156309 (−)	*Epb4.1l4b*	−
57203713-57314709 (−)	*Ptpn3*	low

[1] Genome coordinates are calculated from NCBIM37. + or − indicate strand orientation

[2] Expression deduced from http://biogps.gnf.org